Chapter 5

Calibration Procedure and Performance Specifications

The measurement system described in this thesis is able to measure the gains of multiple propagation channels, calculated the cross-correlation between a pair of gains and calculate the theoretical capacity of a multi-element array system in the measured environment. Noise and mutual coupling between system components can be detrimental to the accuracy of the resulting data. Significant coupling between signals in either the transmitter or receiver subsystems can produce an overestimation of the propagation channels' cross-correlation. Likewise, a low signal-to-noise ratio can reduce the observed cross-correlation and produce equally degraded results. The following calibration measurements provide a high level of confidence that the data integrity of these measurements is not significantly affected by mutual coupling or system noise.

To ensure the accuracy of both the cross-correlation and capacity calculations, the system was designed with a 30dB margin between the signal power and the combined power of noise and coupled-signals. Simulations performed at Lucent Technologies have demonstrated that a measured signal-to-noise ratio of 30dB produces an error margin of 2 bits/sec/Hz and 6bits/sec/Hz at the minimum and maximum MEA capacity values of 10.65 and 106.53bits/sec/Hz, respectively. In this simulation, capacity was calculated

with Equation (3-7) using a system with sixteen transmitters and a system SNR of 20dB. It should be recalled from Chapter 3 that the system signal-to-noise ratio is the predicted value for an ideal communication system and the measured signal-to-noise ratio is defined with the signal power equal to twenty times the log base-ten of the average magnitude of the H-matrix elements. The noise power includes signals from interfering systems and spectral components produced internally by harmonic distortion or coupling. The calibration measurements reports in this chapter were conducted to verify acceptable levels of signal, noise and coupling.

Each calibration measurement was designed to isolate and measure a single system parameter, and compare it to a calculated ideal response. As will be explained in the individual measurement procedures, the following equipment was employed in many of the initial measurements: a Tektronix 2782 spectrum analyzer and a Hewlett Packard 83630A signal generator. The resolution bandwidth of the spectrum analyzer was set to 300Hz, and the internal attenuation of both devices was locked at zero decibels. General references to the spectrum analyzer and signal generator denote these particular components, and additional components are specified as required. For a number of the measurements, the receiver itself is used as a recording device, exactly as it is utilized in a measurement campaign. The procedure for each measurement is presented, as well as the observed results and ideal system response.

In addition to the initial measurements, daily calibrations are required to determine the gains of each signal chain at the time of measurement. System gains vary due to aging and environmental conditions such as temperature and humidity. In addition, permanent variations exist between signal chains because of discrepancies of individual components. For these reasons it is necessary to perform the calibration at the time of the measurement and at the measurement site. During post-processing, the measured gains-matrix is used to normalize the H-matrix data. Together with this daily calibration, the suite of initial tests reported in the chapter substantiates the accuracy of the subsequent measurement campaign.

5.1 Transmitter

The transmitter is characterized by the gain and mutual coupling of the signal chains. An ideal system transmits equal power levels from each antenna, and the signal from each chain contains only the frequency assigned to that particular antenna. Two issues must be noted at this point. First, since the transmitted signal is not modulated, the output power remains constant and amplifier linearity is not a concern in the transmitter calibrations. If the system is later used to transmit data, this issue must be investigated.

Second, because antenna gain is angle-dependant, and because of the difficulties in measuring radiated power in free space, these tests will focus on the antenna input ports. Discrepancies between antenna gains will be recorded in the daily calibrations, as discussed later in this chapter. In view of the consistency produced in modern Printed-Circuit Board (PCB) manufacturing techniques, it is reasonable to assume only small gain variations exist between antenna elements. This assumption is also supported by measurements taken with a similar antenna array inside an anechoic chamber at Lucent's New Jersey facilities, as reported in Chapter 4. Antenna measurements recorded the gain patterns of the majority of elements on a single array, and observed that the differences in the gain between antennas were small, as compared to the magnitude of the antenna pattern ripple.

5.1.1 Transmitter Power

The first test verifies that an equal amount of power is emitted from each transmitter. Equal transmitter powers maximize the receiver's dynamic range. Because dynamic range is defined by the maximum and minimum received signal power required to maintain at least a 30dB signal-to-noise ratio and to prevent harmonic distortion in every transmitted signal, the range is degraded if significant variation exists between the transmitters' output power. This test also guarantees that amplitude variations between two transmitter frequencies in the received signal can be attributed to channel fading and not the transmitters themselves.

All transmitter channels were activated and programmed to produce their predefined frequencies. The spectrum analyzer was used to record the output power from each chain, and the signals were observed to vary no more than 2dB from an average of (–4.0) dBm. This 2dB variation is considerably smaller than the required 30dB signal-to-noise ratio, and will not produce significant degradation of the dynamic range. As with variations in the antenna gain, deviations of this magnitude are normalized by the daily calibration procedure.

5.1.2 Transmitter Mutual Coupling

The next test records the levels of mutual coupling between each pair of transmitter chains. Mutual coupling between internal components in the system produces exaggerated levels of correlation in the final results, and coupled signals must be attenuated at least 30dB below the desired signal level.

A single transmitter output was connected to the spectrum analyzer, and the remaining transmitters were terminated at their respective antennas. All transmitters were activated simultaneously, and the resulting output power at each transmitter frequency was recorded. The observed spectrum consisted of a single desired frequency and multiple coupled tones. This process was repeated sixteen times to observe the output from each transmitter chain. The noise floor, produced by the oscillators' phase noise, was measured as -48dBc, over the system's bandwidth, and no coupled signals were observed above this power level. With a desired signal-to-noise ratio of 30dB at the receiver output, and a flat receiver gain across the 32kHz bandwidth, coupling between transmitter chains will produce negligible errors in the results.

5.2 Receiver

The receiver calibrations expand on the transmitter's gain and coupling tests to include measurements of linearity and the minimum detectable power level. As in the transmitter calibrations, these tests will omit affects produced by the antenna array and observe signals input into the coaxial cables. The receiver tests were used to verify that both the

hardware and software operate within design parameters and produce accurate and precise data. As in the transmitter calibration, all tests are compared to theoretical system performance.

5.2.1 Receiver Gain

This test is similar to the transmitter gain measurement. A gain offset between signal chains would reduce the dynamic range of the system because the minimum and maximum detectable signal levels are limited to that of the signal chains with the lowest and largest gains, respectively.

The signal generator was programmed to output a frequency tone of 2111.004 MHz (equivalent to transmitter chain 2) with a power level of –75dBm. The signal was sequentially input into each of the sixteen receiver chains. It should be noted that this input power level was later verified to be inside the receiver's dynamic range. The receiver was activated, the recorded data processed, and the resulting power spectrum was observed after the Fourier transform calculation. A median gain of 26dB was measured and the remaining chains varied no more than +/- 1dB from this value. Relative to the gain ripple measured in the antennas, gain discrepancies of this magnitude are negligible. This variation is within tolerable limits and should not degrade the system's dynamic range.

5.2.2 Receiver Mutual Coupling

Signal coupling between receiver signal chains will produce exaggerated values of correlation, exactly as between transmitter chains. This test utilized the signal generator and recorded data in the same manner as the receiver gain measurement. A signal was input into the low-noise amplifier of a single receiver chain, and the output spectrum of each adjacent chain was observed. The input signal's power level was increased from an initial power of -90dBm until the frequency tone rose above the noise floor in the adjacent chains. Coupled signals were measured to have power levels attenuated around 50dB when compared to the power in the desired chain. With a specified signal-to-noise

ratio of 30dB, the coupled signal power is well below the noise floor and will not affect the results.

It should be noted that it was necessary to increase the number of samples computed in the Fourier transform to lower the noise floor and observe signal coupling. Also, to prevent damage to receiver components, the input signal power was not raised above –55 dBm if the coupled signal was not easily noticeable.

5.2.3 Receiver Linearity

Signal distortion may be produced by many of the receiver components, and can result in harmonic spurs with power levels comparable to the desired signal. The processing techniques utilized in this system record the amplitudes of specific points on the received spectrum, and harmonic products may be co-located with the desired signals' frequencies. For example, if a 2kHz tone in a specific receiver was distorted and produced harmonics at 4kHz and 6kHz, the recorded data would combine the amplitudes of these harmonics with the desired 4kHz and 6kHz tones. This data would reflect exaggerated levels of correlation between signals from the first three transmitter chains, falsely representing propagation conditions.

Major contributors of harmonic distortion include the audio and RF amplifiers, the analog-to-digital converter and the downconversion mixer. In each of these components, distortion occurs as a result of large instantaneous power levels. In-band spurious components in RF components are usually generated at the third order-intermodulation frequencies. Because of the high RF frequency, ~2GHz, and narrow 32 kHz system bandwidth, second order intermodulation products originating from these components are attenuated in subsequent filtering stages. On the other hand, both second and third order intermodulation products can be generated by the audio components within the receiver's baseband span and may have a large impact on data integrity. Instead of testing each component separately, this test observes the distortion products of the entire signal chain, and measures the highest input power with which the system produces no significant

distortion components. This value will constitute the maximum input threshold for a linear system response.

Two HP8648C signal generators and a Minicircuits ZFSC-2-2500 power splitter were utilized in this test. The two signal generators were programmed to produce 2111.012MHz and 2111.010MHz tones of equal power. These signals were combined in the power splitter and input into a single receiver channel, at the input to the low-noise amplifier. The receiver was activated and the power levels of input frequencies and spurious components were observed from the calculated Fourier spectrum. The power levels of the input tones were then increased from an initial value of –110dBm until the maximum spurious power level rose to -30dB with respect to the power of the input tones. At this point, the input power level was recorded, and the process was repeated for each of the remaining receiver channels. The downconverted frequencies of the 2^{nd} and 3^{rd} order intermodulation products are listed in Table (5-1), where f_1 and f_2 are 2111.012MHz and 2111.010MHz respectively. The intermodulation products of both the RF and audio components are included.

Table 5-1: 2^{nd} and 3^{rd} order intermodulation products of 2111.010MHz and 2111.012MHz as observed in the receiver baseband signal.

f1-f2	2kHz
2f1	20kHz
f1+f2	22kHz
2f2	24kHz
2f1-f2	8kHz
2f2-f1	14kHz
3f2	30kHz
3f1	34kHz

The maximum input power level which produced acceptable distortion was observed as (–55)dBm. With this input level, the maximum spurious power was –31dB below the

desired frequency component. Figure (5-1) depicts the calculated Fourier spectrum produced by the receiver with this input power. As shown in the figure, significant spurious components were observed at the 2nd order intermodulation frequencies. The lower power levels of the third-order intermodulation products suggests that the RF components did not produce significant levels of distortion at this input power. A maximum input power of –55dBm was observed to produce acceptable spurious performance in the receiver.

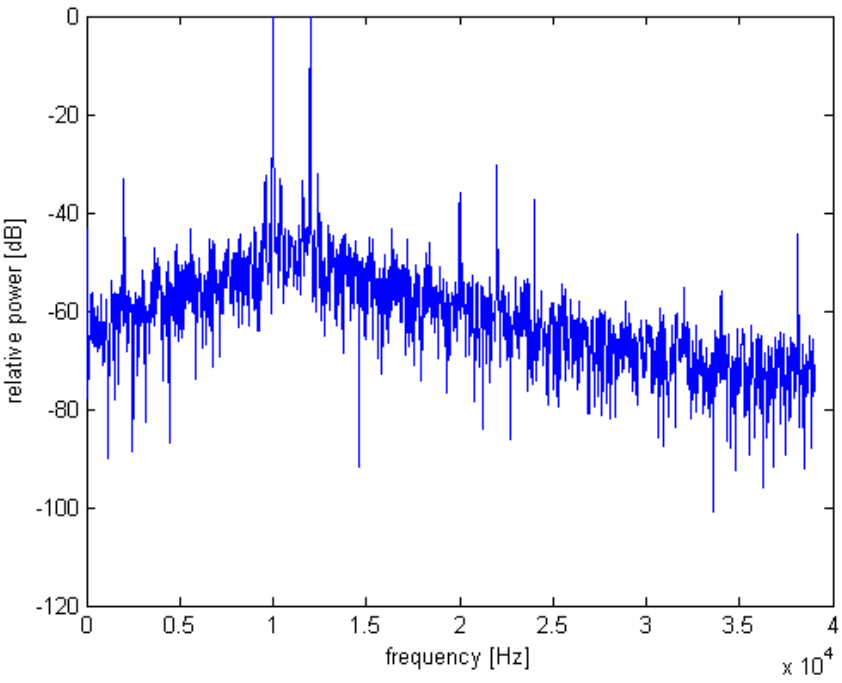

Figure 5-1: Power spectrum calculated from the sampled data recorded by the receiver.

5.2.4 Receiver sensitivity

A minimum signal-to-noise ratio requirement of 30dB was specified in the system design to ensure a high level of accuracy in the MEA capacity calculation. Excessive noise levels can produce reduced correlation and exaggerated MEA capacity results in the data, which do not accurately represent channel fading conditions. A minimum detectable signal power can be measured, below which the receiver does not satisfy the signal-to-noise ratio requirement.

Many of the receiver components can contribute to the noise power of the recorded data. Amplification of the noise by RF components, as specified by the *Noise Figure*, is a consideration in all radio systems. Other factors affecting the signal-to-noise ratio include the resolution of the analog-to-digital converter and the number of samples calculated in the Fourier transform. For this reason, the sensitivity test includes both hardware and software components, and measures the minimum input power necessary to produce the required 30dB signal-to-noise ratio.

The resolution of the analog-to-digital converter (ADC) may limit the signal-to-noise ratio by introducing quantization noise into the sampled signal. Quantization noise is produced when an analog voltage is sampled and converted into discrete voltage levels and may be analyzed by comparing the difference between the discrete voltage and the original analog voltage at each time instant. Equation (5-1) expresses the maximum signal-to-noise ratio obtainable using a ADC with uniform quantization levels. It is assumed that the majority of the noise originates from the voltage errors produced by the DAC and that the input is composed of sinusoidal waveforms [49].

$$SNR_{ADC}[dB] = 6.02(B) + 1.76 + 10\log_{10}(f_S / 2f_{\max}) \qquad \textbf{(5-1)}$$

In this expression, f_S represents the sampling rate, B is equal to the number of bits of resolution, and f_{max} indicates the maximum input frequency of 32kHz. With a 12-bit ADC and a sampling rate of 78125 samples per sec, this expression describes the maximum possible SNR_{ADC} as 74.9 dB [50]. This SNR is achieved when the signal amplitude is equal to the input range of the converter, fully utilizing all of the data bits. This expression can also provide the minimum signal amplitude required to produce a desired SNR. With a required signal-to-noise ratio of 30dB, the peak-to-peak signal level must span at least five bits. This corresponds to an input peak-to-peak voltage of 1.56 millivolts if the full-range of +/-0.1Volts is represented by a total of 12 bits with uniform quantization levels. With a voltage gain of 12 in the audio amplifier, the minimum peak-to-peak voltage at the amplifier input is 0.13 millivolts. This voltage can be transformed into a power of (–64.7)dBm across the 50Ohm input impedance. Including the 23dB

system gain from the antenna output to this point, the minimum detectable level would be (–87.7)dBm if limited by the DAC quantization.

The measured sensitivity may also be compared with a predicted value calculated from the noise figure and gain specifications of the RF components. Table (5-2) itemizes the power budget and lists the gain and noise figure of significant analog components. The gain and noise figure specifications of most components were provided by the manufacturers. Coaxial cable and filter losses were measured with a Tektronic 2782 spectrum analyzer and a Hewlett Packard 83630A signal generator.

Table 5-2: System Power Budget: The left columns list gain and cumulative output power from each transmitter and receiver stage using an estimated free-space path loss. The right side lists noise figure and cumulative noise figure values used to calculate sensitivity.

Transmitter	Gain [dB]	Cum. Pout [dBm]		
DDS (output)		-18.0		
Coax	-0.5	-18.5		
RF LPF	-0.5	-19.0		
RF Mixer	-6.5	-25.5		
Coax	-0.5	-26.0		
AMP	28.0	2.0	distance [m]	100
Coax	-6.0	-4.0	frequency [MHz]	2111
Tx Output Power		-4.0		
Tx Ant. Gain [dBi]	2.0			
Free space Path loss	78.9	◄		
Rx Ant. Gain [dBi]	2.0			
Rx Input Power [dBm]		-78.9		
Receiver			Noise Figure [dB]	Cum. NF [dB]
Coax	-6	-84.9	6	6.00
RF LNA	20	-64.9	1.5	7.50
RF LNA	20	-44.9	1.5	7.51
Coax	-0.5	-45.4	0.5	7.51
RF Mixer	-10	-55.4	10	7.52
RF LPF	-0.5	-55.9	0.5	7.52
			Total Noise Figure [dB]	7.52
			Bandwidth [Hz]	100.0
			Pnoise (Pin) [dBm]	-174.0
			SNRdata required [dB]	30.0
			Sensitivity (Pin.min) [dBm	**-116.5**

In receiver design, the cumulative noise figure is highly dependent on the values of the first components in the signal chain. After the signal is sufficiently amplified, the noise figures of subsequent components are inconsequential to the cumulative value. For this reason, several noise figure parameters were omitted from the table. Equation (4-2) was used to calculate the cumulative noise figure values listed in the far right column.

The receiver's total noise figure can be used to determine the minimum detectable signal power. In equation (5-3), BW denote the system bandwidth as defined by the frequency resolution of the Fourier transform, and SNR_{min} represents the minimum acceptable signal-to-noise ratio of 30dB. The first term of the expression signifies the power spectral density of the thermal noise produced in a 1Hz bandwidth at room temperature. With a total noise figure of 7.5dB, a 100Hz bandwidth and a minimum acceptable SNR of 30dB, this equation results in a minimum input power of (–116.5) dBm, referred to the receiver antenna output. [8].

$$P_{in,\min} = -174 + NF_{TOT} + 10\log(BW) + SNR_{\min} \qquad \textbf{(5-3)}$$

In the sensitivity measurement, the HP8648C signal generator was connected to a single receiver, at the input to the coaxial cable and programmed to transmit a 2111.004MHz tone. This generator is specified to produce a single sideband phase noise of (–110) dBc/Hz at a frequency offset of 20kHz [51]. The input signal power was reduced from an initial value of –70dBm, until the output spectrum from the processed data displayed a 30dB signal-to-noise ratio. This process was repeated for each receiver chain, resulting in a minimum detectable signal of -88dBm. This value represents the minimum detectable signal that was acceptable for all receiver channels. From this analysis and measurement, it can be seen that the resolution of the ADC limited the sensitivity of the system. An audio amplifier with higher gain may improve sensitivity to –116.5dBm, as suggested by the noise figure calculation.

5.2.5 Dynamic Range

The dynamic range of this measurement system is defined by the minimum and maximum power levels which can be input in the receiver while maintaining acceptable performance. Both values have been discussed in the above sections and were measured as –88dBm and –55dBm. Because the measurement system's transmitter produces a constant output power, the dynamic range can be translated into a maximum and minimum allowable distance between the transmitter and receiver antenna arrays, assuming free-space path loss. Although free-space doesn't accurately describe the propagation environment in which this system will be used, the calculation can provide a basic guideline for acceptable performance.

After calculating values of receiver sensitivity and transmitted power, the maximum propagation distance can be estimated using the Friis free space equation. The top half of Table (5-2) describes the gain and cumulative power output provided by the transmitter signal chains. Each signal chain transmits an output power of –4.0dBm, referenced to the antenna input, and both the transmitter and receiver antennas contain an average gain of 2dBi. The Friis free space equation expresses path loss as a function of the propagation distance and signal wavelength, for co-polarized antenna element pairs [11].

$$P_R = \frac{P_T G_T G_R \lambda^2}{(4\pi)^2 d^2} \qquad \textbf{(5-4)}$$

This equation was used to calculate maximum propagation distance over which the measurement system can accurately operate. The maximum propagation distance was found to be greater than 100 meters, more than sufficient in the indoor measurement campaign for which this system was designed. Both the gain and power parameters and the maximum distance of 100 meters are listed in Table (5-2). If a larger distances are required in future measurements, several adjustments can increase the system's range. Modifications may include an additional stage of power amplifiers at the transmitter

output, or the replacement of the coaxial cables at the receiver array to decrease the loss in the receiver front-end. As a note, the distance required to produce a –55dBm power level at the receiver input is 7 meters. In the measurement campaign conducted for this thesis work, the transmitter-receiver separation was limited to this range.

During the measurement process, the received signal power was observed at each measurement location before data was recorded, to ensure the received power was within the system's dynamic range. The majority of the received tones were required to have a power of –80dBm or greater. If only a few tones were measured below this value, it was assumed that the respective antennas were inside a fade, and the measurement could proceed. The signal-to-noise ratio was verified again in the post-processing, and measurements which did not attain the 30dB requirement were discarded. With this procedure, the received power was verified to maintain data accuracy.

5.3 Frequency Synchronization

Frequency synchronization between signal generators and frequency dependent components is important in maintaining the accuracy of the recored data. Frequency dependent components include the direct-digital synthesizers, both the transmitter and receiver local oscillators and the analog-to-digital converters. A frequency shift in any of these components would move the transmitted tones out of their designated frequency bin in the calculated Fourier spectrum. A shift in frequency or phase could change the amplitudes of the quadrature signals recorded in the H-matrix elements.

Phase and frequency synchronization was maintained by referencing all frequency dependent components with GPS receivers. Identical GPS receivers in both the transmitter and receiver subsystem produced an oven-stabilized 10MHz sine-wave output with a typical frequency offset of less than 5e-10, averaged over one second. A calibration measurement of the system's temporal stability, described in the next section, verified that the recorded power of each received signal remained constant for the duration of several hours. This suggested that the shift in transmitted frequencies was sufficiently smaller than the bandwidth of the Fourier transform's frequency bins. In this

measurement, the GPS receivers were found to provide acceptable frequency synchronization in this system.

This system was originally designed to measure both in-phase and quadrature components of the received signals, but due to an unforeseen difficulty in the data acquisition process, the phase information recorded in the data is unreliable. The phase of each H-matrix element was observed to be constant for a duration of ten consecutive H-matrices, and then shifted in the next H-matrix. These abrupt phase shifts occurred at periodic intervals. With 781 samples input into the Fourier transform and a sampling frequency of 78125 samples per second, ten H-matrices represent approximately 0.1 seconds of sampled data. The computer records data to the storage file with this frequency, suggesting that the sampling process is interrupted during recording. A small time lapse in the sampled data could produce the observed phase changes.

This anomaly does not affect the MEA capacity or correlation results reported in this thesis. The cross-correlation coefficient is calculated from the envelope of the received signal, after omitting the phase information. MEA capacity is calculated from a single H-matrix, and abrupt phase changes between H-matrices would not alter individual capacity results. Also, because every H-matrix element is varied by the same amount the phase anomaly is cancelled out in the MEA capacity calculation. The phase of entire matrix is shifted, equivalent to multiplication of the entire matrix by a factor of "$e^{i\theta}$". Equation (4-9) is insensitive to a phase shift over the entire H-matrix, because the phase factor is cancelled in calculating the product of the H-matrix with its complex conjugate transpose. This conclusion is supported in the wired-channel calibrations, from which Figure (5-4) depicts that the calculated MEA capacity remains constant over a stream of measured H-matrices. The observed abrupt phase shifts do not degrade the accuracy of the correlation and capacity results measured with this system.

5.4 Daily Calibrations and Temporal Stability

The method of measuring individual gains of each transmitter and receiver signal chain is described in this section. These values are combined into the gains matrix, and used in

the post-processing in order to correct for small gain deviations between chains. This normalization adjusts the gains to account for variations over time, due to temperature and aging, and also to account for permanent variations between the individual chains. A unique gains matrix was developed for each measurement location, and used for the data taken on that day only. A discussion about the purpose and processing of the gains matrix can be found in the post-processing section of this thesis. The measurement procedure used to produce the matrix is described in this section.

The daily calibration measurements are conducted in a controlled environment, and a probe is placed directly in front of the array under test. The relative gain of each signal channel can be measured if the fading gains between each antenna element and the probe are equal. An ideal free-space channel would produce equivalent fading gains, assuming the separation between the probe and the array is large compared to the largest linear dimension of the array. The following procedure attempts to create this ideal channel while conforming to the spatial restrictions produced involved in indoor calibration measurements.

The gains matrix is calculated from separate measurements of the transmitter and receiver. In finding the transmitter gains, the transmitter was placed in an empty hallway, and all transmitter frequencies were activated. The array was located in the center of the hallway and aligned to make the direction of propagation parallel to the length of the hallway. A probe antenna was then held 1.5 meters from the tested antenna array and moved randomly, orthogonal to the direction of propagation, within a two foot diameter area. The probe antenna was connected to the first receiver channel through a 20dB attenuator, and data was recorded for ten seconds. From this data, the relative gains of each transmitter chain can be calculated. The receiver gains were measured with a similar process. A Hewlett Packard 8648C signal generator was attached to the probe antenna and waved in a two-foot diameter area, 1.5 meters from the receiver array. The generator was programmed to transmit a 2111.004 MHz tone with a –50dBm signal power. Ten seconds of data was recorded from each receiver chain, and the receiver gains were calculated from this data. The system was allowed to operate for a period of

at least one hour before these measurements were conducted, to allow for the components to warm up and for the GPS oscillators to stabilize.

Each gain measurement used a waving motion to collect a representative sample of the signal inside a local area. Ideal gain measurements require a free space environment, such as is produced inside an anechoic chamber. Because calibrations were restricted to indoor locations close to the actual measurement rooms, multipath interference can not be prevented, only mitigated. The potential of large, localized fades exist through the addition of two or more multipath components. By moving the probe antenna over a finite area, the effects of localized fading can be minimized by averaging over a large statistical sample. Ten seconds of data was recorded for each measurement, over which time approximately 1000 separate H-matrices can be computed.

Figure (5-2) depicts the mean and variance statistics of the gains measured during the daily calibrations. Each point in the right-hand graph represents the average gain of one signal chain, over a ten-second measurement. Each point in the left-hand graph represents the variance of the same ten second sample. All signal chains and daily calibration measurements are included in the figure. It can be noted that the majority of the gain distributions contain a variance of less than 0.5dB, demonstrating that the measured gain varied very little even though the probe antenna was waved over a two-foot diameter area. The absence of large signal fluctuations suggests that only the line-of-sight signal lies inside the beamwidth of both the probe and array antennas. If significant multipath components existed, constructive and destructive interference would have resulted in large variance values when the probe was moved over a distance of a few wavelengths.

The mean values in the right side of Figure (5-2) are grouped into receiver (red) and transmitter (blue) chains and centered around a 0dB relative gain value. As discussed in Chapter 3, the H-matrix is normalized by its total power before it is input in the MEA capacity calculation, and the correlation coefficient is normalized by the average value of

the inputs. Only the relative gain between signal chains is necessary to produce accurate estimates of correlation and MEA capacity.

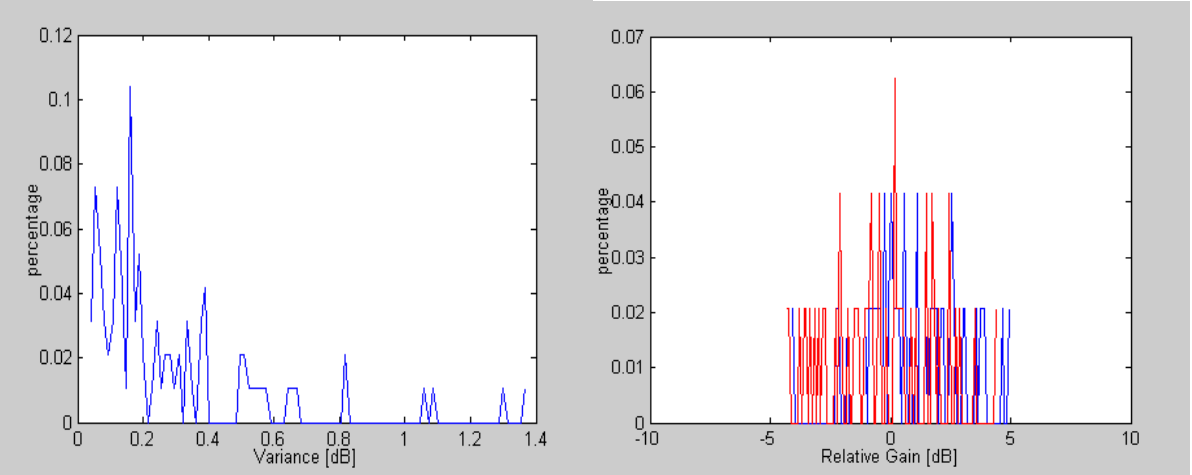

Figure 5-2: Distribution of the mean and variance values of the received power for the daily calibrations. Each mean or variance value represents the statistics of gain over a ten second measurement for a single channel at a single measurement location.

The presence of both horizontal and vertical polarized elements in each of the transmitter and receiver antenna arrays complicated the daily calibration measurement. In order to analyze accurately the channel gains, two sets of data were collected for both the transmitter and receiver arrays. The probe antenna was aligned with horizontal polarization for the first dataset, and vertically polarized for the second. In processing the calibration data, the horizontal and vertical channels were found separately from their respective data and combined to produce a complete channel list. This method allowed for an accurate measurement of array elements with varying polarizations.

A measurement was also conducted to determine the length of time over which a calibration measurement was accurate. The system was set up in an empty hallway and measurement data was collected at three hour intervals for a period of eighteen hours. The data was then processed and the average H-matrix was found for each ten-second measurement. The measurements were then compared to determine the time interval over which all elements remained relatively constant. Over a twelve hour time span, the average received power from each channel varied less than 2dB. Because actual

measurements take between five and seven hours per location, this test determined that only one calibration is necessary to process all of the data taken for each location.

The gains-matrix from each daily calibration is used to normalize the measured data after it has been processed into an H-matrix form. The calibration adjusts the gains of each signal chain to account for temporal or permanent gain biasing. Equal gains at both the transmitter and receiver are required to obtain accurate estimates of both correlation and MEA capacity.

5.5 Wired Keyhole and Singleton Channels

Wired channel measurements are useful in determining the upper and lower measurable limits of channel capacity using this system. The propagation environment is produced by attaching coax cables between the transmitter and receiver subsystems. In such controlled propagation environments, measurement data can be compared with theoretical results to evaluate system performance.

The *wired keyhole* and *wired singleton* channels produce the theoretical lower and upper capacity limits respectively, and are produced with the transmitter and receiver arrangements depicted in the following figure. In the keyhole measurement, all channels collapse into a single path and all H-matrix elements are fully correlated. The transmitter signal chains are combined using a 16/1 splitter, attenuated, and then split into the sixteen receiver inputs. The only source of decorrelation originates from noise generated internally from system components. The ideal measurement system produces an all-ones H-matrix in this propagation environment and results in the minimum MEA capacity, as described in Chapter 3.

The wired singleton channel simulates a high-multipath environment, in which the propagation channels are uncorrelated. This calibration test records the highest MEA capacity values measurable by the system. An ideal system produces the identity matrix with diagonal matrix elements equal to one and all other elements equal to zero. This matrix maximizes the MEA capacity as calculated with Equation (3-13). To produce this

propagation channel, each transmitter signal chain is attenuated and attached directly into a single receiver chain.

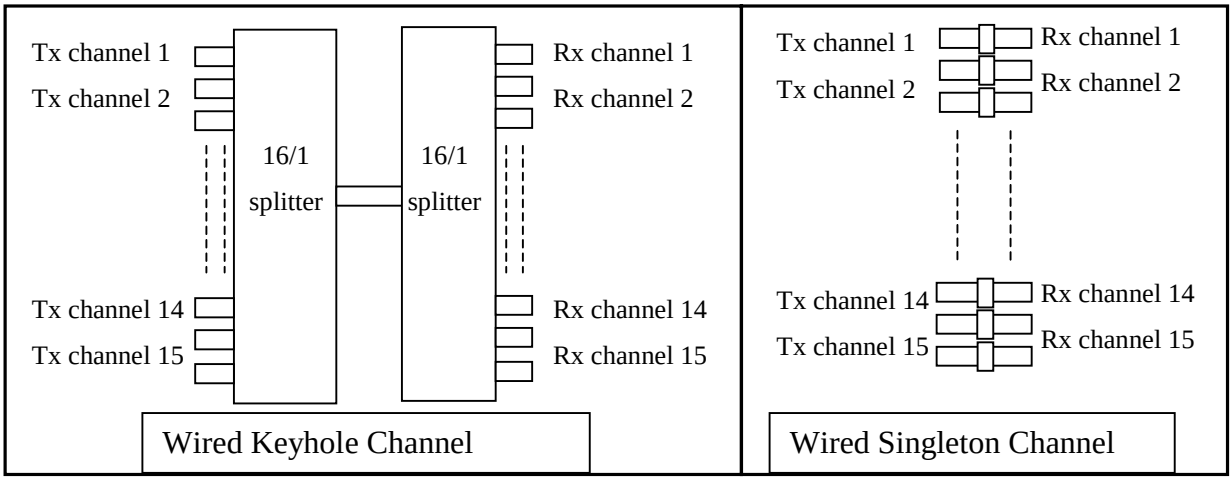

Figure 5-3: Cable arrangements between the transmitters and receivers, producing the wired keyhole (left) and wired singleton (right) channels. All signals pass through a single cable to produce the keyhole channel, and all of the signal paths are independent in the singleton channel.

Figure (5-4) depicts the high and low limits of MEA capacity obtainable with this system as well as the theoretical limits as calculated with ideal H-matrices. The theoretical limits of 10.65 bits/sec/Hz and 106.53 bits/sec/Hz were calculated by substituting the all-ones matrix and the identity matrix into Equation (3-13), after normalization. The lower bound is equivalent to the capacity of a single antenna, and the upper bound represents the fully potential capacity of a similar sixteen antenna system in ideal propagation conditions.

The measured limits have average values of 12 bits/sec/Hz and 103 bits/sec/Hz. These results are consistant with simulations conducted at Lucent Technologies, which predict the error in MEA capacity due to non-ideal H-matrices produced by a measurement system with 30dB SNR. The simulations predicted that a 30dB SNR produces an error of 2 bits/sec/Hz at the minimum capacity and 6 bits/sec/Hz at the maximum capacity level. The difference between measured capacity levels and the ideal limits is less than the

errors predicted by the simulation, suggesting that both noise and correlation between signal chains is above the acceptable limits. Also, the wired-channel measurements confirmed that the measurement system is able to produce an large range of capacity values.

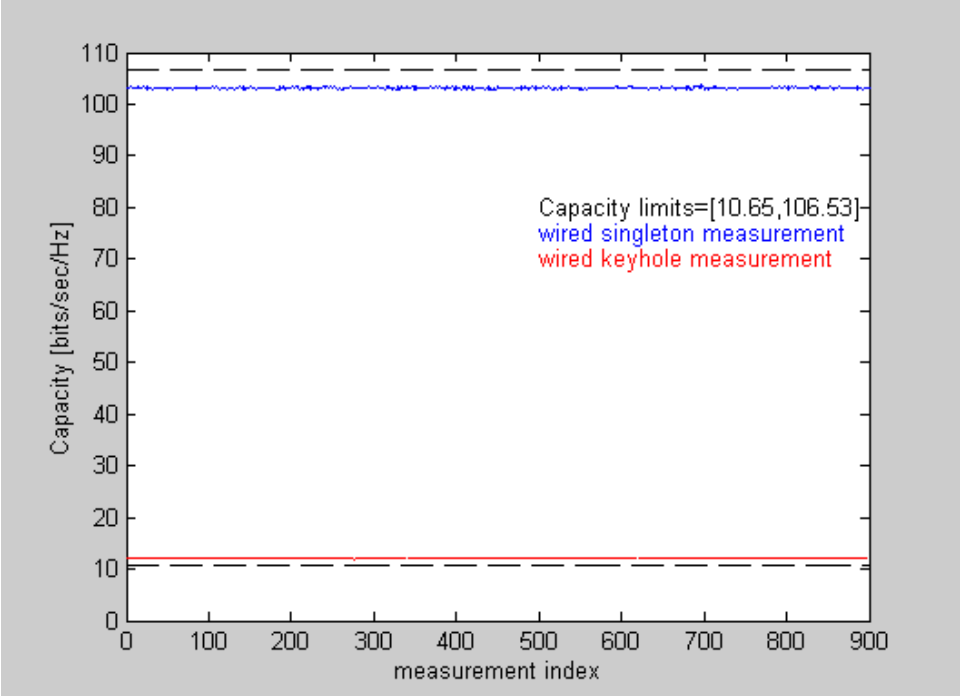

Figure 5-4: Measured capacity values in the wired keyhole (red) and wired singleton (blue) channels. The theoretical upper and lower capacity values (black) were calculated from the identity matrix and the all-ones matrix, respectively.

5.6 Free-Space Measurement

System performance in an ideal free-space environment should mimic the results measured with the wired keyhole channel, but system response changes dramatically with the addition of spatially separated channels, and mutually coupled antennas with practical beamwidth, gain and polarization characteristics. Array parameters such as antenna spacing and mutual coupling determine the minimum and maximum achievable system capacities, in much the same manner as they affect diversity performance. The following discussion focuses on the free space measurement, and explains a number of the details

nirvana that can increase system capacity beyond the ideal minimum value. This measurement provides a baseline capacity value for systems using arrays with the following characteristics.

These particular arrays each contain sixteen elements, evenly divided into vertical and horizontal polarizations. This polarization diversity reduces the correlation between many pairs of array elements, and results in an increased MEA capacity. In free space, the system should result in two independent sub-systems, each containing eight transmitters and eight receivers. The minimum theoretical capacity for this scenario can be calculated using Equation (3-13), to be 19.3 bits/sec/Hz. It should also be noted that the maximum theoretical capacity does not change from the single polarization case. For an ideal free space channel, a theoretical capacity value of 19.3 bits/sec/Hz should result from this measurement, instead of the 12 bits/sec/Hz measured in the wired keyhole calibration.

This theoretical capacity calculation does not account for non-ideal channel and antenna characteristics which would further increase the minimum value. Although a measurement location was selected to represent the ideal free space environment, a small number of scatterers exist in any practical setup. Signal correlation was demonstrated by Lee to depend on the arrangement of scatterers and the spacing between array elements. Lee demonstrated that even in the environment of a high cellular base-station, a finite antenna spacing can produce decorrelated propagation channels. Additional sources of decorrelation can be derived from the rippled antenna gain pattern and finite beamwidth observed in Chapter 4. These characteristics increase the measured capacity in the "near" free-space environment, above the theoretical value. The purpose of conducting a measurement in this environment is to provide a minimum capacity limit for the system with these particular arrays. It should be noted that this uncontrolled environment provides only a rough estimate of this minimum capacity; an anechoic chamber would produce a more exact estimate.

The selected free space environment was located in the front parking lot of Durham Hall, and measurements were conducted at times when large sections of the parking lot were empty. Non-ideal aspects of the location included lampposts located approximately 50 meters apart and several small trees separated by the same distance. The transmitter and receiver were arranged 30 feet apart in an area away from these obstacles. A large transmitter-receiver separation was selected to prevent coupling affects between the two arrays and ensure the validity of the free-space models. The Fraunhofer distance was used as a guideline to confirm this distance [11]:

$$d_f = 2D^2/\lambda \qquad \textbf{(5-5)}$$

In this calculation, "D" is the largest linear dimension of the antenna. A conservative estimate of this distance uses the diagonal of the entire array as the largest distance and results in a Fraunhofer distance of eighteen feet.

An additional precaution was used to verify a free space environment. The volume around the line-of-sight path can be divided into several Fresnel zone regions, defined by the radii at the observed point on the path. Scatterers located at the boundaries of each region can produce multipath components at the receiver that contain a pi/2 phase offset with respect to the line-of-sight signal. These components may destructively interfere with the line-of-sight signal and produce signal fading. The propagation environment approaches the ideal free space model, as scatterers are removed from a greater number of Fresnel zones. The radius of the nth Fresnel zone is calculated Equation (5-6) [11]:

$$r_n = \sqrt{\frac{n\lambda d_1 d_2}{d_1 + d_2}} \qquad \textbf{(5-6)}$$

In this expression, the distances "d_1" and "d_2" refer to the distance from the transmitter and receiver respectively of the observed point along the line-of-sight path. It should be noted that the radius is largest when the two distances are equal and the observed point is halfway between the transmitter and receiver arrays. In this location the closest

scattering obstacle is the ground. With the bottom of the array at a height of ten feet, no scatterers are located in the first ten Fresnel zones.

In the parking lot environment, the arrays were arranged facing each other with a separation of thirty feet and a height of ten feet. After the previously discussed daily calibration procedure, two ten second measurements were recorded, resulting in minimum, mean, and maximum values of system capacity of 37.9, 38.5 and 39.2 bits/sec/Hz respectively. Because of the absence of scattering objects, the free space channel provides the worst-case scenario for a multi-antenna system. Except in specific cases, the capacity of a system using a particular pair of antenna arrays will always improve with the addition of scatterers. For this reason, a system designer may use the results of a free space measurement as a benchmark in evaluating array designs. This environment provides an estimate of the minimum capacity provided by a particular pair of antenna array.

This chapter has presented the calibration procedure and results used to verify system performance. Initial measurements observed gain, coupling and dynamic range parameters of the individual signal chains. Subsequent tests involved predictable environments and determined the measurable range of MEA capacity as limited by noise and coupling in the system. Wired channel measurements demonstrated the ability to measure approximately 95% of the theoretical capacity range. The final free-space measurement found a baseline capacity estimate, which includes affects originating from the antenna arrays used in this investigation. This baseline capacity has significance in system design and will be used as a minimum capacity value in data analysis.